DESIGN AND FABRICATION OF A ROADSIDE VERTICAL AXIS WIND TURBINE

A final year project report

Presented to

SCHOOL OF MECHANICAL AND MANUFACTURING ENGINEERING

Department of Mechanical Engineering

NUST

ISLAMABAD, PAKISTAN

In Partial Fulfillment

of the Requirements for the Degree of

Bachelors of Mechanical Engineering

by

Abdul Sami Syed

Abdul Wahab Sajid

Haseeb Uddin Ahmed

June 2018

EXAMINATION COMMITTEE

We hereby recommend that the final year project report prepared under our supervision by:

ABDUL SAMI SYED	NUST201432768BSMME11114F
ABDUL WAHAB SAJID	NUST201432714BSMME11114F
HASEEB UDDIN AHMED	NUST201433495BSMME11114F

Titled: "DESIGN AND FABRICATION OF A WIND TURBINE" be accepted in partial fulfillment of the requirements for the award of BE-MECHANICAL ENGINEERING degree.

Supervisor: Dr. Zaib Ali, Assistant Professor SMME, NUST	Dated:
Committee Member: Dr. M. Sajid, Assistant Professor SMME, NUST	Dated:
Committee Member: Dr. Emad Uddin, HOD SMME, NUST	Dated:

_____ _____

(Head of Department) (Date)

COUNTERSIGNED

Dated: _____ _____

(Dean / Principal)

ABSTRACT

This report describes the proceedings of the final year project; in partial fulfillment of the bachelor's degree at School of Mechanical and Manufacturing Engineering, NUST, H-12, Islamabad to design and fabricate a straight bladed vertical axis wind turbine for roadside deployment which should be able to generate enough power to sustain the streetlights and aims at extracting energy from the wind gusts generated as a result of passage of vehicles on the roadside.

With the ever growing energy demand, it has become necessary to carry out research in renewable energy technologies. The report presents a thorough overview of the potential estimation of wind at the side of the roads, suggests ideal location for application of wind turbine to harness energy. The details of the turbine design and optimization are also provided.

A brief account on the methods used to manufacture the turbine is also provided. Testing of the turbine was done in limited circumstances, yielding satisfactory results but there is still room for further improvement in the design.

PREFACE

This final year project report describes the designing and fabrication aspects of our vertical axis wind turbine. This project was done considering the ever-growing need of renewable energy sources for fulfilling the power demand of the country. It harnesses energy through the otherwise-wasted energy i.e. road side wind gusts generated through passage of traffic. Further research and development of the design needs to be done before installation on a large scale.

ACKNOWLEDGMENTS

We would like to acknowledge the support; both monetary and moral, of our parents, and our mentor, Dr. Zaib Ali, who have been there for us throughout this project. We would also like to acknowledge the help of Umar Farooq, for helping us out in the algorithm development of Double Multiple Stream Tube model on MATLAB, and the efforts of Ahmed Wahaj for his help in order to find the dynamometer of our desired power range. This project might not have been possible without their support.

ORIGINALITY REPORT

We hereby confirm that work included in this report is our own except for the works cited.

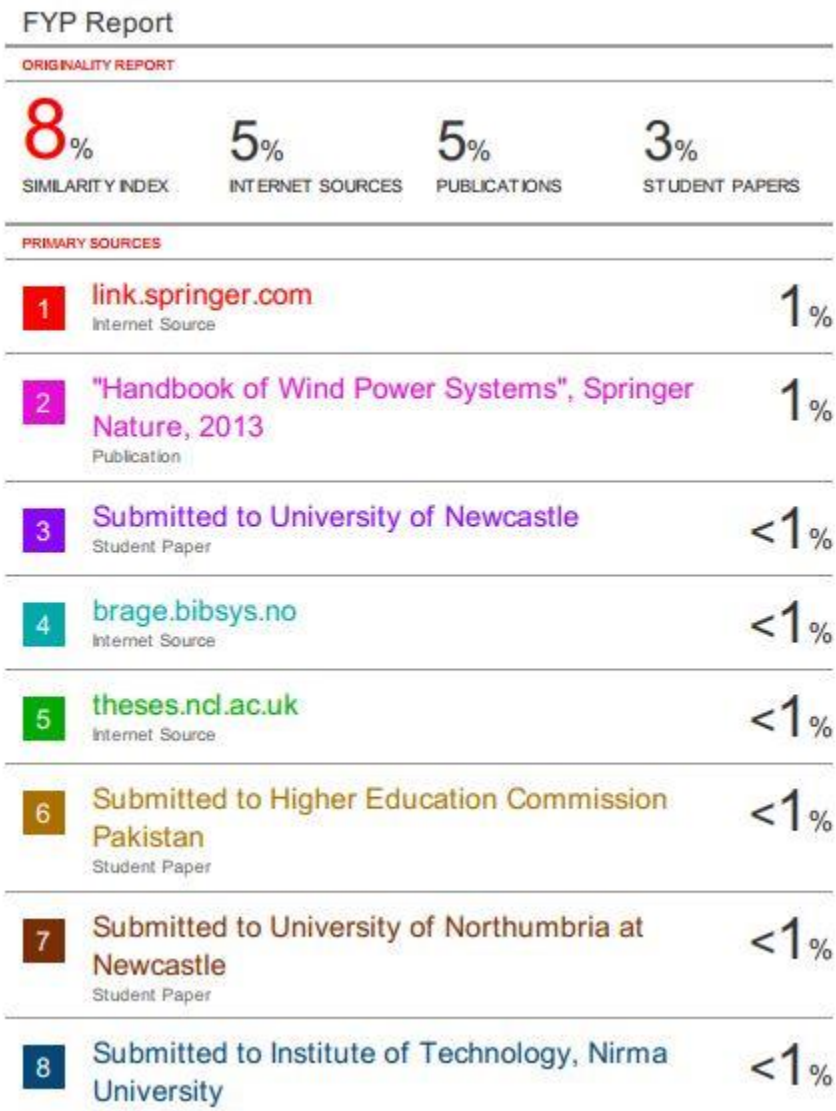

FYP Report

ORIGINALITY REPORT

8%	5%	5%	3%
SIMILARITY INDEX	INTERNET SOURCES	PUBLICATIONS	STUDENT PAPERS

PRIMARY SOURCES

1	link.springer.com Internet Source	1%
2	"Handbook of Wind Power Systems", Springer Nature, 2013 Publication	1%
3	Submitted to University of Newcastle Student Paper	<1%
4	brage.bibsys.no Internet Source	<1%
5	theses.ncl.ac.uk Internet Source	<1%
6	Submitted to Higher Education Commission Pakistan Student Paper	<1%
7	Submitted to University of Northumbria at Newcastle Student Paper	<1%
8	Submitted to Institute of Technology, Nirma University	<1%

_____

Project Supervisor

(Dr. Zaib Ali)

__ June, 2018

COPYRIGHT

TABLE OF CONTENTS

ABBREVIATIONS

AEDB	Alternative Energy Development Board
USPCAS-E	U.S. Pakistan Centre for Advanced Studies - Energy
HAWT	Horizontal axis wind turbines
VAWT	Vertical axis wind turbines
NACA	National Advisory Committee for Aeronautics
TSR	Tip Speed Ratio
DMST	Double Multiple Stream Tube
CFD	Computational Fluid Dynamics
SMME	School of Mechanical & Manufacturing Engineering
NUST	National University of Sciences & Technology

NOMENCLATURE

α	Angle of Attack (deg)
σ	Solidity
ρ	Density of air (kg/m^3)
ω	Rotational Speed (rad/s)
λ	Tip Speed Ratio
C_d	Drag Coefficient
C_l	Lift Coefficient
C_p	Performance Coefficient
C_q	Torque Coefficient
A	Swept Area (m^2)
V	Velocity (m/s)
l	Blade length (m)
C	Chord length (m)
N	Number of Blades
P	Power (W)

CHAPTER 1

INTRODUCTION

With growing advancement in the technology and the gradual increase in urbanization, a shift to renewable energy sources is not only recommended for a better and safer environment but also a need of the hour. The fossil fuels are depleting very fast, and the situation demands the utilization of alternate sources of energy. In addition, they also contribute in higher amounts of carbon in the environment resulting in global warming. This situation in addition to the ever-increasing energy demand, drives the need for a greater research in renewable energy sources all over the world. Our project deals with harnessing the wind energy to generate electricity, the concept which is not very prevalent in Pakistan. The generated electric power is intended to light the light poles on a highway.

1.1-Motivation for Work

The renewable energy sector in Pakistan is highly underdeveloped. Pakistan still produces a major chunk of its electric power from fossil fuels. With growing increase in demand, and the shortfall affecting the country's economy and standard of living, it has also impeded in the development of industry in the country. So it is necessary to find out better and sustainable ways of generating power. The increased research and investment in the green energy will also help in fighting global warming and pollution.

Pakistan being a member of Paris Climate accord, vows to take steps, adopt measures and regularly report its contribution in the control of global warming. Pakistan making almost two-thirds of its power grid from fossil fuels, is contributing to the increase in overall global carbon print. The member countries of the accord are bound to reduce their carbon output to reduce the global warming.

The renewable energy sources leave no carbon print in the atmosphere, thus they do not contribute in any kind of environmental hazards. Converting from the hazardous fossil fuels to the green energy sources which are environment friendly and sustainable at the same time, will act as a stepping stone to a power-sufficient and developed Pakistan.

Table 1.1: Overall cost analysis of different energy sources [1]

Energy Source	**Price (USD)**	**Fuel usage (USD/h)**	**Maintenance cost**	**Life (years)**	**CO_2 (g/l)**	**NO_2 (g/l)**
Solar panel (1 kVA)	632	0	0	25	0	0
Gas generator (1 kVA)	1067.50	1.08	0.06	3 – 5	6.4	58
Wind turbine (1 kVA)	1165.44	0	0.03	12 - 15	0	0

The table clearly depicts that the renewable energy sources are friendly for the environment by not letting any hazardous gases in the atmosphere. It also shows that renewable energy sources are more sustainable, not only having a greater life but are also much more financially feasible.

Wind energy rose to the attention of the world in 1970s following the oil crisis. The need for finding alternative sources of energy increased as a result of Harrisburg and Chernobyl nuclear reactor accidents in 1980s. The world focus shifted to containing the amount of gases emitted into the atmosphere during 1990s. All of these factors paved way for the development and research of wind energy [3].

European countries took the initiatives of launching programs explicitly focused on research and development of wind energy. The market for wind turbines has ever since been growing as can be observed from the following table that documents the installation of new wind energy plants and total capacity of various countries:

Table 1.2: Global wind power capacity in 2017 (MW) [18]

Country	Installed in 2017	Cumulative in Dec 2017
PR China	19,500	188,232
USA	7,017	89,077
Germany	6,581	56,132
UK	4,270	32,848
India	4,148	23,170
Brazil	2,022	18,872
France	1,694	13,759
Turkey	766	12,763
Mexico	478	12,239
Belgium	467	9,479
Rest of the World	5,630	83,008
Total	**52,573**	**539,581**

Pakistan, having 792 MW of cumulative wind power capacity in Dec 2017, unfortunately has not been able to keep up with the increasing trend of research and development in the wind energy sector, which was one of the reasons why we decided to build a wind turbine as our final year project.

1.2- Wind Turbines

Turbines convert kinetic energy of fluid into rotational energy through rotor and that energy is transformed into electrical energy by means of a generator.

1.2.1-Classification of wind turbines

Wind turbines are, in general, classified on various basis, e.g. by the axis about which the rotor blades rotate. According to this criteria there are two categories of wind turbines:-

- Horizontal axis wind turbines
- Vertical axis wind turbines

Another criterion that can be used to classify wind turbines is the location of the rotor relative to the tower and nacelle:

- Upwind
- Downwind

Wind turbines are also classified by the mechanism that rotor blades use to achieve the rotation and thus create electricity, following are the types of turbine according to this criterion:

- Lift type
- Drag type

Most commercial turbines today are three bladed, lift type, horizontal axis wind turbines with the upwind rotor [1]. Our wind turbine is a lift type VAWT, so we now shift our focus to VAWTs only. VAWTs are primarily categorized into following categories:

- Savonius rotor (Drag type)
- Darrieus turbine (Lift type)
- Giromill (Lift type)

Darrieus rotor uses aerodynamic lift forces to achieve rotation and has the shape of an egg beater, whereas the Giromill (sometimes casually referred to as Darrieus) is also a lift type VAWT and is a modification of the Darrieus rotor, the only difference between the two is that the Giromill has straight blades.

Our application requires us to convert the energy from the disturbance caused in the air by the moving vehicles into electrical energy, a decision was made that for this application, Giromill would be the most suitable rotor, and the reasons for this decisions will be elaborated in the following chapters. For now, we will focus mainly on Giromill or straight bladed VAWT.

1.2.2-Components of a Wind Turbine

A wind turbine (Giromill in particular) primarily is a combination of the following main components:-

1. Rotor
2. Nacelle
3. Foundation and Tower

1.2.2.1-Rotor

Rotor consists of the frame that rotates as a result of wind, with rotor blades that are attached to the shaft with the help of connecting links, since we are talking about a lift type VAWT, the blades used are NACA airfoils. The rotor is mounted on a hub that is in turn fixed to the shaft for power transmission to the generator in order to convert the energy into electrical power.

1.2.2.2-Nacelle

A housing that collectively holds generator, power control mechanism (can either be mechanical or control systems). For VAWTs the nacelle can be on the ground, making VAWTs relatively easier to maintain as compared to HAWTs in which the nacelle has to be at the top of the tower.

1.2.2.3-Foundation and Tower

Foundation is used to support the tower and the whole structure of the wind turbine in order to ensure structural integrity of the turbine as a whole. Tower is usually a hollow tube through which the shaft passes.

1.2.3-Efficiency of a Wind Turbine: Important Parameters

This section highlights the important parameters that affect the performance of turbines.

1.2.3.1-Performance Coefficient

The efficiency of a wind turbine is determined by various parameters. We start by stating the available potential in wind, which is given by [3]:

$$P_{wind} = \frac{1}{2}\rho A V^3 \tag{2.1}$$

Where P is power, ρ is density of the air, A is the swept area of the rotor and V is the incident freestream velocity. From this available power, a wind turbine can extract the following amount [3]:

$$P_{turbine} = \frac{1}{2}C_p\rho A V^3 \tag{2.2}$$

Where, C_p is the performance coefficient of the rotor. The maximum value of performance coefficient is given by Betz limit as 0.593 [3]. Commercial three bladed HAWTs have achieved a C_p of up to 0.45 whereas VAWTs reach up to 0.35 [3] as shown in figure 2.1.

1.2.3.2-Tip Speed Ratio

Tip speed ratio (TSR) is defined as the ratio of the speed of the tip to incident freestream velocity, given as:

$$\lambda = \frac{\omega R}{V} \tag{2.3}$$

Where λ is the TSR, ω is the radial velocity in rad/s and R is the rotor radius.

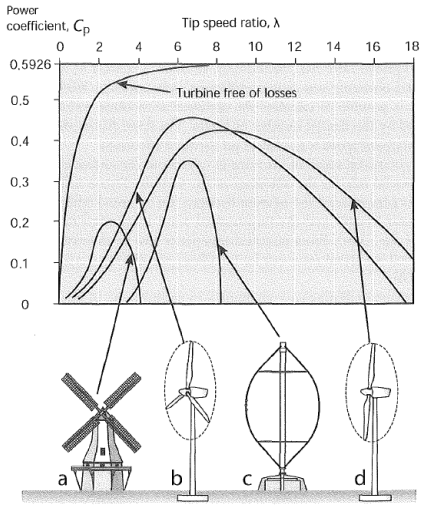

Figure 2.1: Performance Coefficients of various turbines [3]

As can be seen from this figure, C_p varies with TSR.

1.2.3.3-Swept Area

Swept area is the area swept by the rotor blades and it directly affects the amount of power that can be extracted from the wind, increasing swept area increases power but it also increases cost, so a balance between the two is made where the amount of power can justify the cost incurred.

1.2.3.4-Airfoil

Since, we are talking about lift type turbines, the turbine blades are airfoils, mostly NACA airfoils. For the Omni directionality of VAWTs, the airfoils used are mostly symmetrical airfoils NACA00XX [4]. Aerodynamic analysis of these airfoil blades at specified Reynolds numbers is necessary for performance prediction and design optimization methods. The choice of a correct airfoil for a particular application is very crucial to the

performance of a wind turbine. At optimum angle of attack (α), an airfoil generates maximum lift and minimum drag as shown:

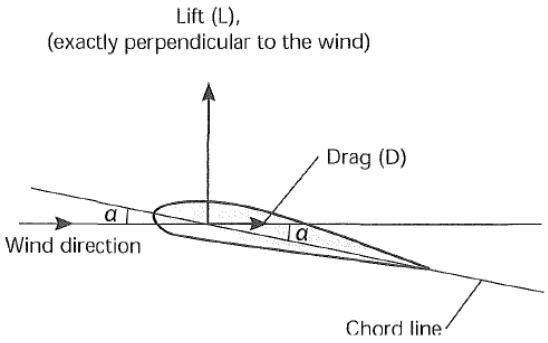

Figure 2.2: Airfoil: Lift and Drag Forces [3]

1.2.3.5-Solidity

Rotor solidity is defined as the developed surface area of all blades divided by the rotor swept area, this is a key variable and greatly affects the performance and the cost of the turbine [4]. Solidity is given as:

$$\sigma = \frac{Ncl}{A} \tag{2.4}$$

Where, σ is the solidity, N is the number of blades, c is the chord length of the airfoil, l is the length of the blade and A is the swept area.

1.2.3.6-Problem Statement

With already a limited electric power available in Pakistan, road lights and street lights use a reasonable portion of the grid. This chunk of energy can be utilized in the industry or other sectors if these lights are powered through an alternate source. This source can be a solar cell or a small scale wind turbine. Solar powered cells are already being used for the purpose of powering the road lights. The idea to introduce a wind turbine for the purpose is strengthened by the following facts:

- Solar cells have power conversion efficiency much lower than the wind turbines. The highest attained efficiency for the multi-junction cells in the laboratory conditions is 46% [2] while the efficiency attained in the actual conditions is much lower. While the commercial wind turbines can have the power conversion efficiency of up to 50%.
- Wind can be harnessed all day and night, while the solar cells cannot generate power at night or in cloudy conditions.
- Wind turbine can be placed such that to attain greater incoming wind velocity as a result of wind gusts produced by the moving cars.

These points affirm that installing a wind turbine will be a very reasonable idea for power generation for the road lights.

1.3-Objectives of the Project

The objective of the project is to develop a vertical axis wind turbine designed for the running in the wind gusts produced by the traffic on a busy highway. The project also aims to fabricate a full scale turbine, which can be reduced to a scale model if proper funding cannot be procured.

The objectives of the project can be enumerated as:

1. To select a proper site on or near a highway for designing the turbine based on the parameters like wind velocity and available potential at the site.
2. To design a Giromill type Vertical Axis Wind Turbine using DMST model.
3. To design and manufacture the foundation to support the turbine.
4. To perform structural analysis of the model including stress analysis.
5. To select and install already available generators in the market for the conversion of mechanical energy to electrical energy to power the road lights.

CHAPTER 2

LITERATURE REVIEW

A detailed study of literature was done prior to the design and fabrication of model. A summary of the literature that was reviewed is presented in this section and is later applied in the next chapter.

Tore Wizelius [3] described the types, basic working, relevant parameters and components involved in all wind turbines.

Parascivoiu [4] explains the performance of Darrieus type VAWT. All the parameters involved in the performance of a Darrieus rotor are presented in detail along with their effects on the overall performance of the turbine. Especially, the Double Multiple Stream Tube model later used to predict and optimize the performance of our turbine, is mostly adapted from the chapter 6 of this book.

A scaled prototype for the desired application was manufactured [5]. The senior design project was mainly concerned with the bearing design and airfoil selection optimization for the said application. It was concluded that NACA 0018 was the optimum airfoil for this application.

Another prototype designed for conditions similar to roadside was manufactured [6]. Another methodology used for the design of the small scale VAWT is decribed. The airfoil used was NACA 0021.

Effects of aspect ratio (H/R) of the rotor on the performance of the rotor are discussed [7]. It is concluded that lower aspect ratio for an identical rated power, yields more power as compared to the rotor with higher aspect ratio. But, the resulting gain in performance coefficient is very small.

The effects of various design parameters; chord, number of blades, Re number etc. on the performance of the rotor are discussed [8]. The prominent result for this kind of application is that the efficiency gain for 4 blades compared to 3 blades is not as big as shifting from 2 to 3 blades. So, three blades offers a marginally good efficiency at a reasonable cost for our application.

Numerical approach is used to predict the performance of VAWTs [9] based on Double Actuator Disk theory and Momentum models and is compared with results obtained from Computational Fluid Dynamics, the results are fairly close and thus both techniques for performance prediction are equally reliable.

Various possible configurations are reviewed [10]; Savonious, Darrieus, Giromill, Straight bladed, Egg beater shape. It is concluded that a straight bladed Darrieus rotor or a Giromill would be the most suitable option for this application.

Economic aspects of small scale site specific wind turbines are reviewed [11]. The results from this paper also favors a three bladed rotor.

The effects of pitch angle of airfoil on the performance of the rotor is explained [12]. Having a variable pitch would be highly beneficial in terms of total power produced by the turbine, as in commercial HAWTs. But, the design configuration of VAWTs makes it relatively tedious to vary the pitch.

The difficulties involved in the self-starting of VAWT are discussed [13]. It is concluded that a Savonius-Darrieus Hybrid may be used for the turbine to have the self-starting capability.

The effects of unsteady winds on the performance of the VAWT are discussed [14]. For the roadside application, unsteady wind gusts affect the performance of wind turbines.

A small scale wind turbine with self-starting capability was manufactured [15]. Various parameters to improve the efficiency are discussed. Again, three blades were used for the application.

All the literature review helped in understanding the working of VAWT and suggested measures to improve the efficiency and self-starting capability of the turbine.

CHAPTER 3

METHODOLOGY

This chapter focuses on the methodology and the thought process employed to go about this project.

3.1-Project Plan

Our project was conducted using the strategy shown below:

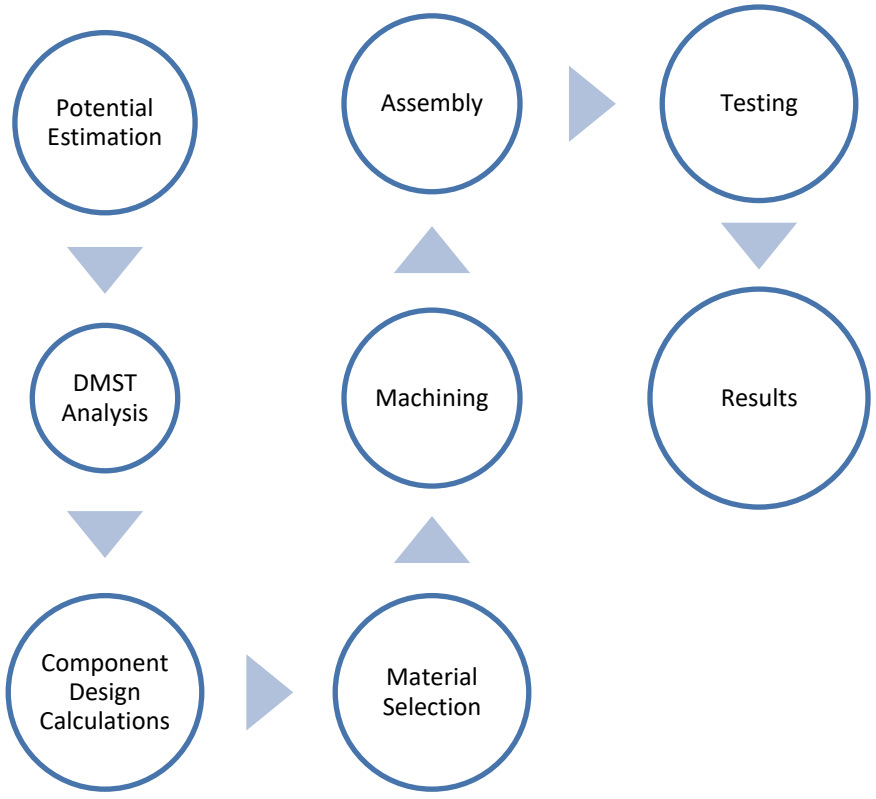

3.2-Site Potential Estimation

The first step, which had to be done before starting the design of our wind turbine was to estimate the potential available in wind gusts that are generated when a vehicle passes by. A general observation and intuitive idea is that the bigger the vehicle, greater would be the disturbance caused by it, thus more velocity in air. Higher the velocity of the wind, higher would be the wind potential according to Eq. 2.1.

3.2.1-Experimental Data

In order to estimate the available potential, a hot wire anemometer was used to measure the roadside wind speed. The ideal site would be a two lane road on each side with consistent traffic even on moderate speed with road divider in the middle which should have a width of 2 meters. These numbers are not guess work, they were obtained from calculations which will be revealed as we go along this chapter.

Samples were collected on various locations at a rate of one sample every 5 seconds, between 5:00 pm and 7:00 pm when traffic is thought to be steady. The results obtained are given in table 3.1.

Table 3.1: Roadside Experimental Wind Data

Location	No. of Samples	Sampling Description	Maximum velocity	Minimum Velocity	Average Velocity
Kashmir Highway (G-10)	12	Dense traffic	5.66	2.31	4.48
Kashmir Highway (G-10)	51	With & without traffic	3.51	0.17	1.35

Kashmir Highway (G-9)	37	With & without traffic	4.55	0.25	2.04
Zero Point Bridge	99	With & without traffic	3.93	0.22	1.90
Islamabad Expressway (G-8)	99	With & without traffic	4.52	0.25	2.63

As can be seen from this data, Islamabad Express Way is more suitable for our application, and these values are from late hours on a weekend, the traffic peak hours during peak days ought to have higher velocities. Thus, our application site's potential was validated from these results.

3.2.2-ANSYS Fluent 2D Simulations

To further strengthen the argument that our site would have enough potential to justify the installation of a wind turbine, 2D simulations were conducted on ANSYS Fluent 18.1 for side view and top view of a Toyota Corolla. The dimensions for Toyota Corolla were obtained from internet. Using these dimensions and a sketch, top view and side view of the car were made in Solidworks, which were later imported to ANSYS.

A standard lane width of 3.7 m [16] was used to design the simulation boundary, 5 lanes were incorporated in the top view simulation. For the side view a height of 10 m was used as the height of enclosure. K-epsilon model with two equations was used in the analysis with realizable wall functions [19]. The results obtained are shown in figures 3.1 to 3.4.

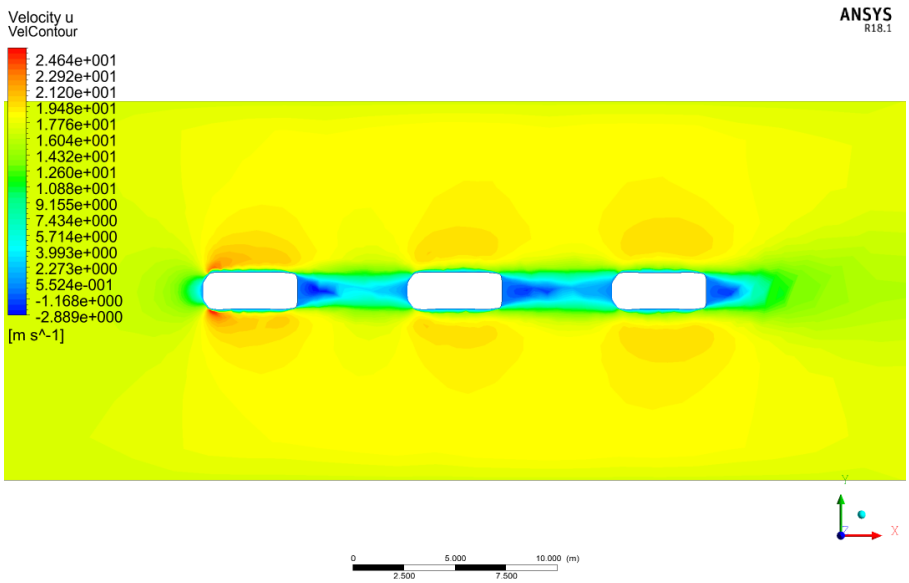

Figure 3.1: ANSYS Fluent 2D Simulation: Top View Velocity Contours

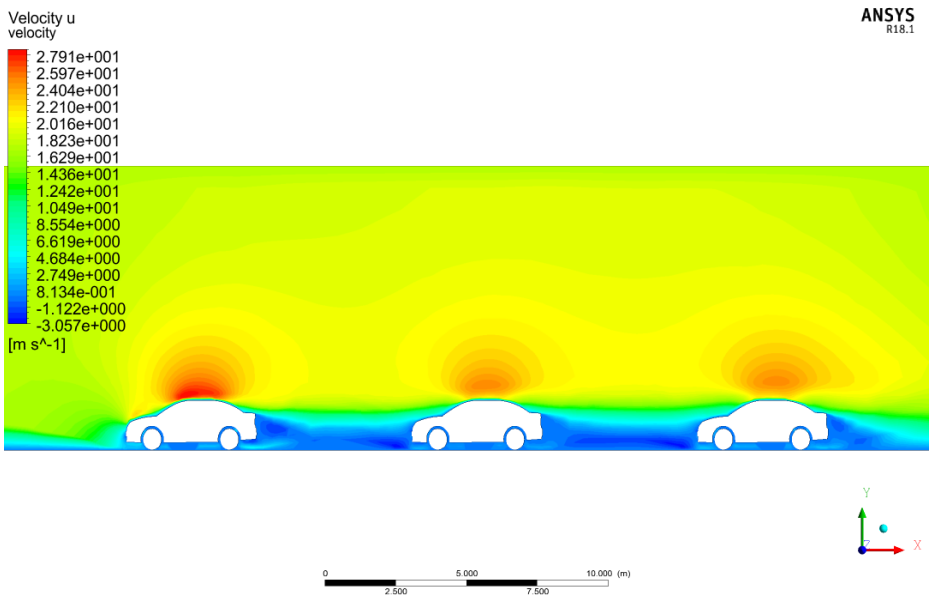

Figure 3.2: ANSYS Fluent 2D Simulation: Side View Velocity Contours

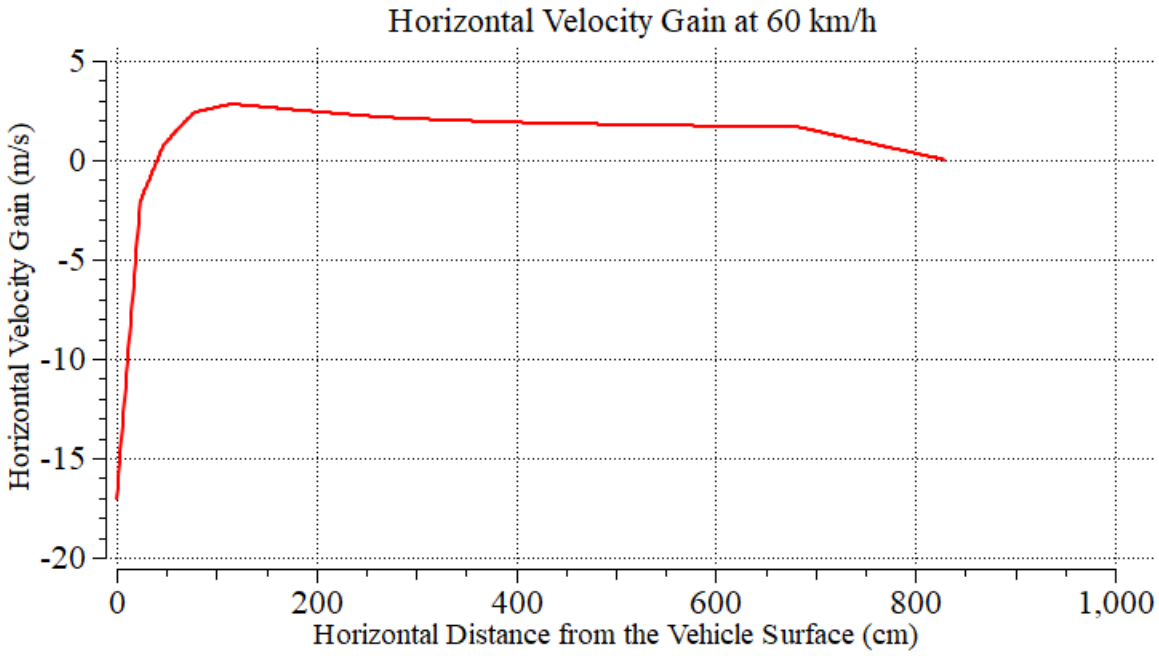

Figure 3.3: ANSYS Fluent 2D Simulation: Velocity gain in Horizontal direction

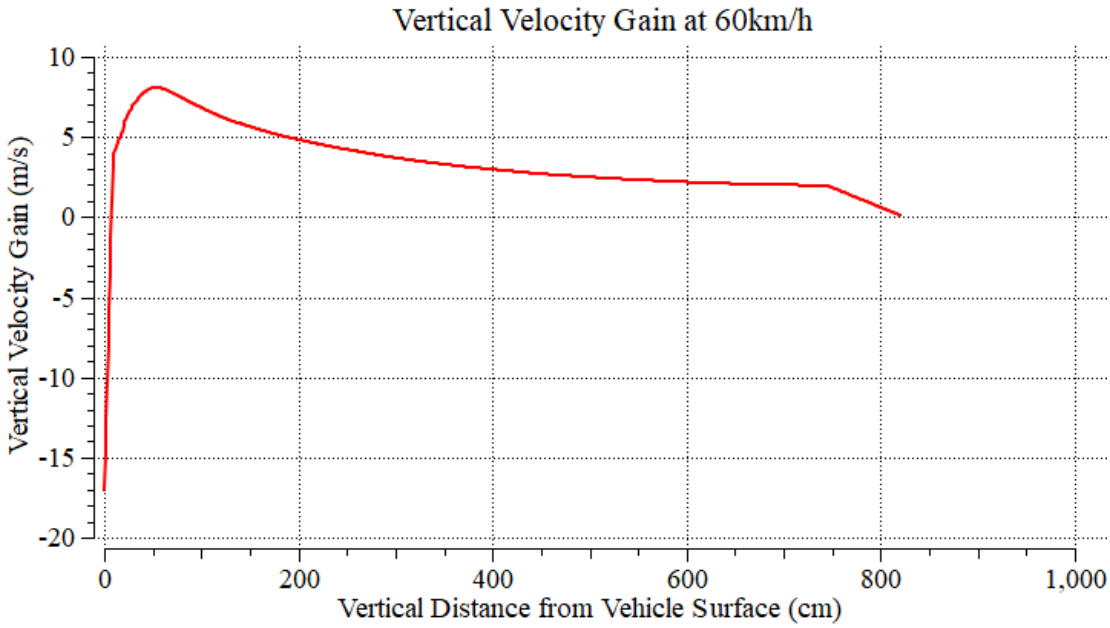

Figure 3.4: ANSYS Fluent 2D Simulation: Velocity gain in Vertical direction

These results are from the simulations that were conducted at 60 km/h, which is a moderate velocity, the innermost lane on roads usually reaches 100 km/h. The noticeable thing in these graphs is that after passing the boundary layer due to the attachment of the flow with the surface of the vehicle, the velocity gain rises to a max at a distance of approximately 0.5 m from the surface of vehicle and then fades away as the distance increases.

These results are in agreement with the data that was collected experimentally using hand held anemometer. To predict annual power production by a turbine, the frequency distribution of the wind must be known. To determine frequency distribution on the site, a cup type anemometer at the desired hub height with a data logger must be used. This project is not funded yet, thus unfortunately, we were not able to do that.

3.3-Turbine Parameters Calculation

This section details the reasoning used to justify the design decisions.

3.3.1-Straight Bladed VAWT

Straight bladed VAWT was preferred over the conventional egg beater shaped rotor for two reasons:

- Manufacturability
- Lesser swept area for same height
- Cost

With the resources that were at hand, it would have been difficult to manufacture curved blades, and it would also have incurred more cost. Moreover, for two rotors with same height and diameter, the swept area of the Darrieus rotor $(2/3)D^2$ is lesser than its Giromill counterpart, thus straight bladed alternative offers more extractable power. So, it was decided to go with the simpler straight bladed Giromill rotor.

3.3.2-Rated Power and Rated Wind Speed

In an average day, the traffic on the roads is consistent from 6:00 am till 10:00 pm, in general. So, it can be expected that the turbine will generate most of its power for sixteen hours. The power generated in the remaining hours would be relatively low.

Whereas, the LED street lights remain on for twelve hours a day on average. The power rating of LED Street light varies from 50 W to 150 W. So, the power consumption per day is calculated.

Energy consumed = $P.t$ = 150 x 12 = 1800 Wh = 1.8 kWh

Corresponding to this power consumption, an iterative procedure, assuming a C_p of 0.3, at an average wind speed of 6 m/s for 16 hours was used to find the required area.

$$A = \frac{Energy\ Consumed}{0.5\ C_p \rho V^3 t} = \frac{1800}{0.5 \times 0.3 \times 1.2 \times 6^3 \times 16} = 2.89 \sim 3\ m^2$$

So, a swept area of 3 m^2 is needed in order to completely offload a Street light from the power grid.

The rated power for this turbine at a rated wind speed of 10 m/s would be 540 W ~ 500 W.

3.3.3-Rotor Dimensions

To achieve a swept area of 3 m^2, there were various sets of lengths and radii that satisfied this requirement, but keeping in mind the width of the road divider, it was decided to have a rotor length of 2 m and a rotor diameter of 1.5 m.

$$A = l \times D = 2 \times 1.5 = 3\ m^2$$

3.3.4-Number of Blades

As mentioned in chapter 2, various papers that were reviewed favored the use of three blades. Fewer blades with larger chord are a better choice than more blades with smaller

chord, for the same value of rotor solidity [4]. Four blades also mean more cost. Thus, a decision was made to use three blades.

3.3.5-Airfoil

As mentioned in chapter 2, various papers that were reviewed favored the use of NACA 0018 airfoil for our application.

3.3.6-Solidity and Blade Chord Length

For structural integrity a minimum chord of 0.1 is necessary [4]. Thus, minimum acceptable chord length using Eq. 2.4 comes out to be 5 cm. Since, this parameter directly affects both performance and cost directly. The higher the chord; thus higher solidity, higher would be the cost. An iterative procedure outlined in [7] was used to settle for an initial chord length value of 13 cm; on the basis of results obtained from DMST performance prediction algorithm. So, the solidity using Eq. 2.4 is:

$$\sigma = \frac{Ncl}{A} = \frac{3 \times 0.13 \times 2}{3} = 0.26$$

3.4-Performance Prediction and Design Optimization

An adaptation Double Multiple Stream Tube model presented in Parashivoiu, Chapter 6 [4] that uses the convergence point between Double Actuator Disk theory and Blade Element Theory to predict the performance of VAWTs, was used for performance prediction and design optimization.

The performance at five different solidities was analyzed ranging from 0.1 to 0.5, and at TSR between 0.5 and 12. An averaging scheme was used to determine five different local Reynolds numbers; at which the analysis were to be conducted, corresponding to five different chord length values. MATLAB code shown in Appendix II was used to determine the optimum chord length.

The following graphs were obtained from QBlade:

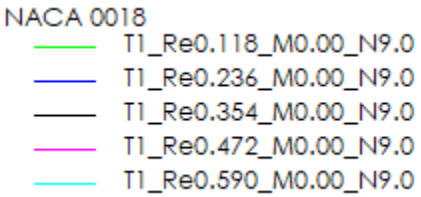

Figure 3.5: Legend for images from QBlade

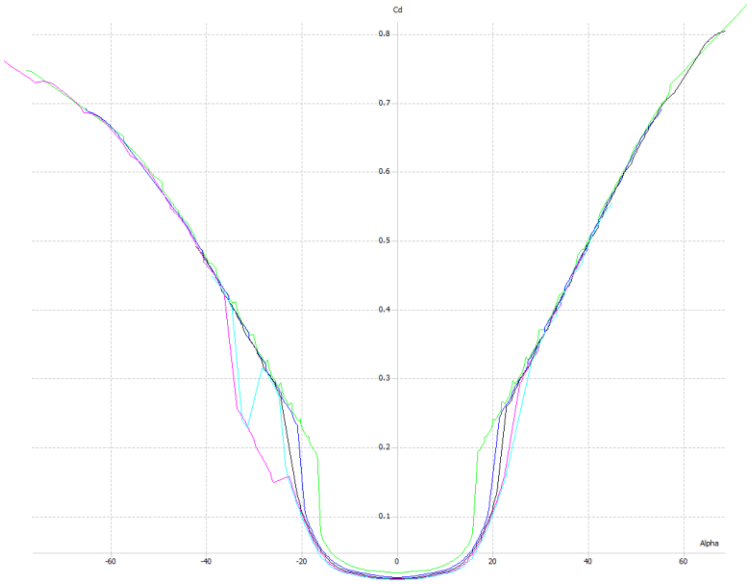

Figure 3.6: C_d vs α from QBlade

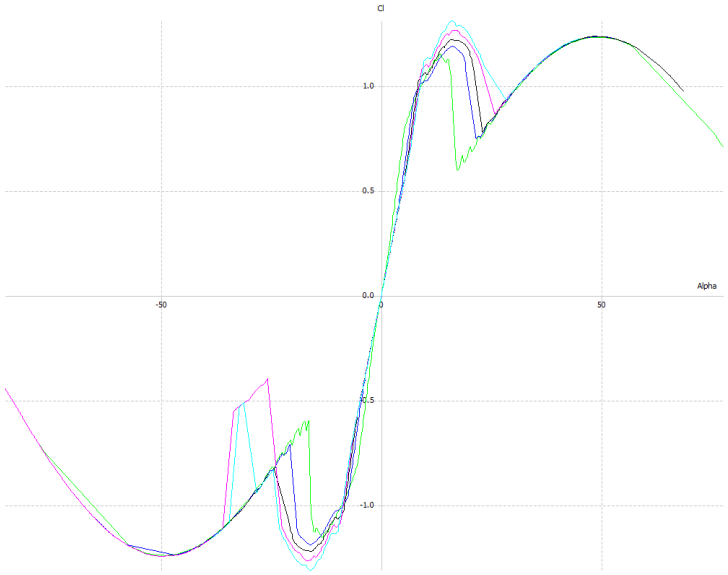

Figure 3.7: C_l vs α from QBlade

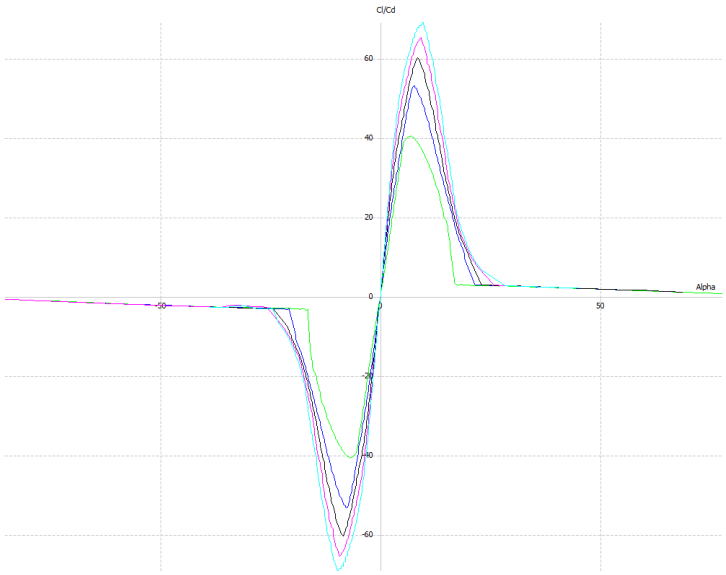

Figure 3.8: C_l/C_d vs α from QBlade

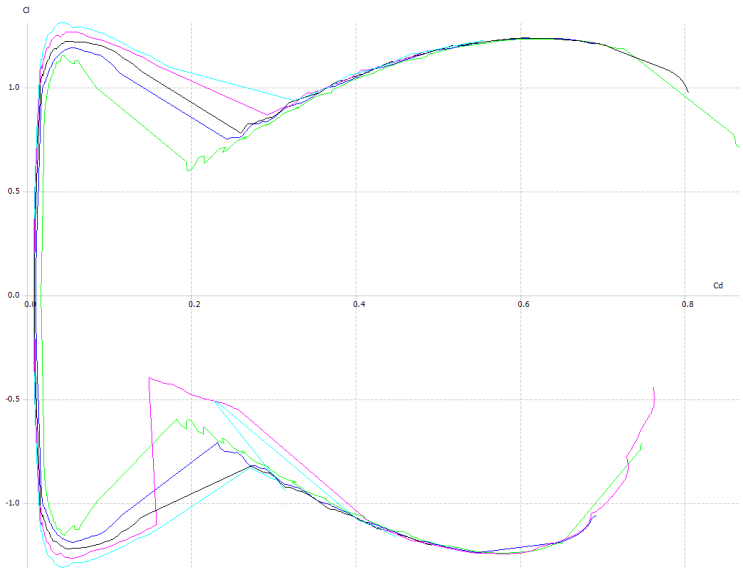

Figure 3.9: C_l vs C_d from QBlade

Using the MATLAB code, a graph was obtained which shows an optimum chord length of 14 cm.

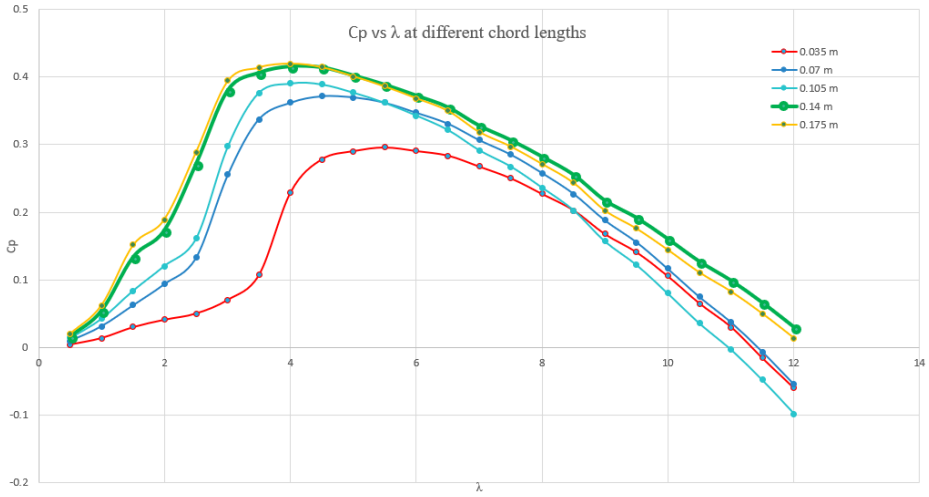

Figure 3.10: C_p vs λ at different chords

3.5-CAD model

A 3d-model was drawn in Solidworks. This was used for stress analysis in ANSYS.

Figure 3.11: CAD model of the turbine

3.6-Stress Analysis

The cutoff speed of turbine is set to be 20 m/s. The DMST analysis at 20 m/s result in maximum tangential and normal forces that the rotor would have to face. Maximum torque that the shaft would have to transmit is also available from this analysis at cutoff wind speed. Considering these forces, the selection of materials for rotor is done. Shear stress and bending moment diagram are drawn for the shaft in order to calculate the reaction forces. Maximum shear stress and maximum normal stress theory are used to determine the dimension of our shaft as well as the radial arm. After the dimensions are selected, the weight of the rotor components is determined which is used to select bearing. Calculations can be found in Appendix III.

Results of stress analysis of frame on ANSYS have been shown in Appendix IV.

3.7-Fabrication

After the stress analysis, the process of fabrication required us to find the most cost-effective materials available in the market which could bear the forces and pressure exerted on them.

3.7.1-Material Selection

For this purpose, Aluminum 6061 was used as the material for steel and for fabricating the hubs, and radial arm-blade connection sleeves. Stainless steel was considered for radial arms, nuts, bolts, washer and foundation frame.

Table 3.2: Material Properties of the used materials

Material Properties	**Aluminum 6061-T6**	**Stainless steel**
Tensile yield strength (MPa)	276	215
Shear strength (MPa)	310	291
Elastic modulus (GPa)	68.9	200
Density (kg/m^3)	2700	8000
Machinability	Good	Poor
Corrosion Resistance	Excellent	Excellent

3.7.2-Airfoil Blade

The manufacturing of the blade proved out to be the most troublesome part. A pattern for blade was created first through CNC wood carving of 40 wooden pieces of 1-inch depth. Glass fiber was selected as the material for the blades due to its low density and high strength (150 MPa).These pieces were cleaned by rubbing sand paper and joined using

special glue to form a 1 m pattern. A mold was then formed using three glass fiber sheets, epoxy resin and separating wax for each blade. Consequently, three hollow blades of glass fiber were manufactured.

Figure 3.12: Rough wooden pieces

Figure 3.13: Glued pieces for forming pattern

3.7.3-Bearing Selection

SKF Bearings 6206-2Z, the energy efficient deep groove ball bearings, were considered after meticulously calculating radial and axial forces, and weight of the rotor on the bearing. These bearing exhibit ultra-low friction and offer an excellent way to reduce

energy consumption. It is cooler compared to SKF standard bearing at equivalent loads and speeds, reducing lubricant use and potentially extend the life of equipment. The bearing is also caged so that any dirt or water is prevented from reducing the life of the bearing.

3.7.4-DC Generator

A DC permanent magnet generator (dynamo) was coupled with the shaft for harnessing the power. Permanent magnet generator's advantage over the electromagnet generator (alternator) is its ease of starting without any energy requirement. The generator is rated at 500 W i.e. the maximum power the turbine can be produce is equal to the rated power of generator given that it can sustain the wind speed loads at that condition.

3.7.5-Belt Drive Mechanism

Generator and shaft are coupled using belt drive mechanism comprising of two cast iron pulleys having a gear ratio of 1:5 connected through an A type V-Belt. Belt drive provides a noiseless smooth transmission of power.

Figure 3.14: Wind Turbine Model

CHAPTER 4

RESULTS AND DISCUSSIONS

The turbine was tested in two ways:

1. By simulating the roadside conditions by the use of room coolers.
2. Placing the turbine on the top of load deck of a pickup van.

4.1-Simulation of roadside conditions

It was necessary to test the turbine in the conditions for which it was designed. The necessary permissions could not be acquired from the relevant highway authorities, so an alternate method had to be adopted. The required flow conditions were produced by placing the room coolers in a counter flow arrangement.

Figure 4.1: Arrangement for producing flow conditions similar to the roadside flow conditions

Although the flux of the incoming air could not be managed to cover even half of the total area of rotor, but the test gave a pretty clear picture of the cut-in wind speed for the wind turbine. The wind speed incoming from the cooler was measured with the help of a vane type anemometer, perpendicular at the face of rotor area. Wind speed came out to be 4.9 m/s.

Figure 4.2: Measuring Wind speed

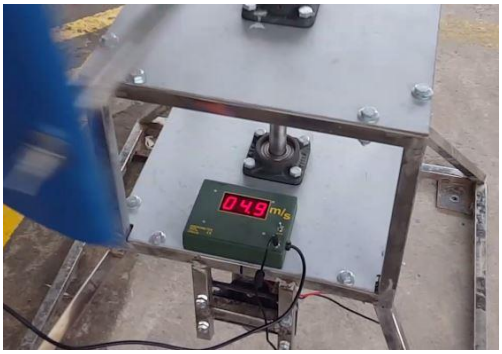

Figure 4.3: Calculated Speed

4.1.2-Cut-in Wind Speed

As a wind tunnel of such a large scale could not be found, cut-in wind speed for the design conditions had to be calculated from the aforementioned arrangement. Before the coolers started to give wind at the maximum speed, the turbine started to rotate at almost 4.5 m/s wind speed. Therefore it is apparent that the turbine will have a cut-in wind speed of somewhat less than 4.5 m/s when it is placed in the road side conditions where the flux provided to the rotor will be maximum, unlike the simulated conditions.

4.2-Turbine placed on the top of load deck of pickup van

The turbine was also tested by placing it on the top of load deck of a moving pickup van. In this way the turbine was tested by simulating the conventional wind tunnel conditions.

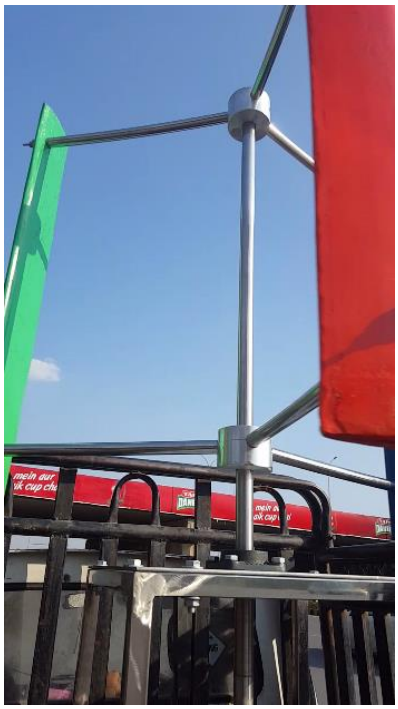

Figure 4.4: Turbine on the load deck of a pickup van

The turbine was placed in a way so that the incoming wind faces the rotor area perpendicularly. Wind speed was set by controlling the speed of pickup van and was measured using a hot wire anemometer.

Table 4.1: Results at a wind speed of 7 m/s

Description	Value
Up Stream Wind Speed (m/s)	7
RPM of Turbine	195
RPM of Generator	975
Voltage (V)	29.6
Current (I)	1.45
Power (W)	42.92

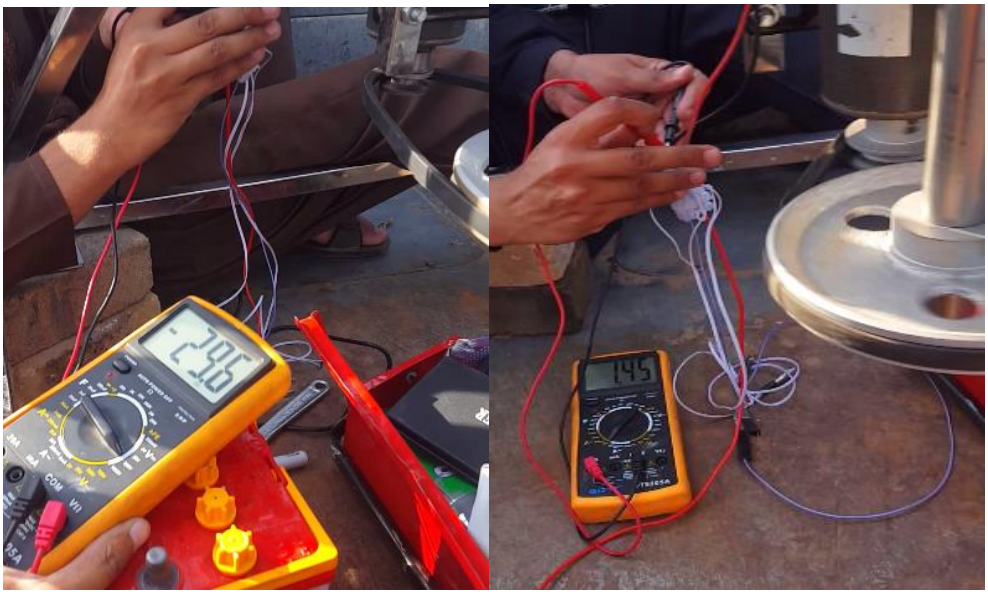

Figure 4.5: Measurement of Voltage (left) and Current (right) at wind speed of 7 m/s

In this way various turbine performance parameters were calculated.

Table 4.2: Experimentally calculated Turbine Parameters

Description	Value
Available Power at 7 m/s (W)	202.37
Power Output at 7 m/s (W)	42.92
Co-efficient of Performance - C_p	0.212
Tip of the blade Speed (m/s)	10.21
Tip Speed Ratio - TSR	1.46

4.3-Discussion

- Turbine produces enough power at the design speed to charge the battery for powering LED street lights at night time.
- Experimentally calculated co-efficient of performance is in line with the theoretically calculated one at the design wind speed.
- Tip-speed ratio is not completely matching with the predicted TSR at the design stage but it can be understood that there are always deviations of the fabricated model from the ideally designed model according to DMST by Paraschivoiu [4].
- Rated power of the turbine is 500 W as it is dependent on the rated power of the generator attached. The power is bound to increase exponentially as the wind velocity is increased.

CHAPTER 5

CONCLUSIONS AND RECOMMENDATIONS

5.1-Conclusions

The project was completed and met the deliverables successfully. Following conclusions can be derived:

1. The idea of capturing the wind gusts coming from the traffic at highways is proved to be viable.
2. DMST modelling is an efficient way of designing the turbine.
3. The turbine is expected to produce 156 KWh of electrical units annually if it is placed in an upstream wind speed of 7 m/s for at least 10 hours a day.
4. The turbine was tested in extreme conditions of 17 – 18 m/s in the stormy conditions, and the turbine proved to have structural integrity even when rotating at very high RPMs.
5. The blades made of glass fiber, being very light weight, proved to be a good choice in material selection as they are capable of coping with high wind speeds.

5.2-Recommendations

Following points are recommended for the future work in this area:

1. The design can be used on the highways being newly built and can be incorporated on the light poles by integrating them at the appropriate height. In this way the cost of the frame can totally be eliminated, making the turbine financially viable.
2. Feasibility can be further improved by procuring an appropriate generator of only such rated power which will be later produced while in function. Generators of higher rated powers cost much more and the same job can be taken from a generator of just enough rated power.

3. Variable pitch angle can be incorporated in the design for the efficient performance of the turbine.
4. Further research on hybrid savonius-darrieus turbine for the road-side application is highly recommended, as it can further improve the self-starting ability.

WORKS CITED

[1] Khalil H.B.; Zaidi J.H. (2014). Energy crisis and potential of solar energy in Pakistan (pp. 194 – 201)

[2] Dimroth, F.; Tibbits, T.N.D.; Niemeyer, M.; Predan, F.; Beutel, P.; Karcher, C.; Oliva, E.; Siefer, G.; Lackner, D.; (2016). Four-Junction Wafer Bonded Concentrator Solar Cells, IEEE Journal of Photovoltaics (pp. 343–349)

[3] Wizelius, T. (2016). Developing wind power projects: theory and practice. Routledge (p. 5, 19, 48, 66, 68, 70, 74, 78)

[4] Paraschivoiu, I. (2009). Wind turbine design: with emphasis on Darrieus concept. Montréal: Presses internationales Polytechniques (p. 365)

[5] Dennison, M.; Gutierrez, E.; Moore, E. (2016). Vertical Axis Wind Turbines for Collection of Highway Wind Energy

[6] Castillo, J. (2011). Small-scale vertical axis wind turbine design

[7] Brusca, S.; Lanzafame, R.; Messina, M. (2014). Design of a vertical-axis wind turbine: how the aspect ratio affects the turbine's performance

[8] El-Samanoudy; M & A. E. Ghorab; A & Z. Youssef. (2010). Effect of some design parameters on the performance of a Giromill vertical axis wind turbine.

[9] Beri; Habtamu & Yao; Yingxue. (2011). Double Multiple Stream Tube Model and Numerical Analysis of Vertical Axis Wind Turbine

[10] Bhutta; Muhammad & Hayat; Nasir & Uzair Farooq; Ahmed & Ali; Zain & Rehan Jamil; Sh & Hussain; Zahid. (2012). Vertical axis wind turbine - A review of various configurations and design techniques

[11] Saeidi; Davood & Sedaghat; Ahmad & Alamdari; Pourya & Alemrajabi; Ali Akbar. (2013). Aerodynamic design and economical evaluation of site specific small vertical axis wind turbines

[12] Rezaeiha; Abdolrahim & Kalkman; Ivo & Blocken; Bert. (2017). Effect of pitch angle on power performance and aerodynamics of a vertical axis wind turbine

[13] Hill, N.; Dominy, R.; Ingram, G.; Dominy, J. (2008). Darrieus turbines: The physics of self-starting

[14] Danao, Louis & Eboibi, Okeoghene & Howell, Robert. (2013). An Experimental Investigation into the Influence of Unsteady Wind on the Aerodynamic Performance of a Vertical Axis Wind Turbine

[15] Bansil, J.A.; De Guzman, J.B.; Mayote, K.; Reyes, M.A.; Tiu, R.J.L. (2014). Development of a Darrieus-type, Straight-blade Vertical Axis Wind Turbine Prototype with Self-starting Capability

[16] Bani-Hani, E., Sedaghat, A., AL-Shemmary, M., Hussain, A., Alshaieb, A. and Kakoli, H. (2018). Feasibility of Highway Energy Harvesting Using a Vertical Axis Wind Turbine. Energy Engineering, 115(2), pp.61-74.

[17] Lane. (2017, November 23). In Wikipedia, The Free Encyclopedia

[18] Global Wind Statistic 2017. (2018). Global Wind Energy Council, Brussels.

[19] Feng, G.; Haidong, W.; Hui, W. (2017). Comparison of different turbulence models in simulating unsteady flow.

APPENDIX I: TURBINE PARAMETERS

Description	Value
Swept Area (A)	1 m^2
Blade Length (H)	1 m
Rotor Diameter (D)	1 m
Rated Power (P)	500 W
Rated Wind Speed (V)	10 m/s
Cutoff Wind Speed (V_c)	20 m/s
Chord Length (c)	14 cm
Solidity (σ)	0.41
Number of Blades	3

APPENDIX II: MATLAB CODE

The following code was written and used to determine the local Reynolds numbers:

```
clear all; clc;
nu = 1.48*10^(-5);
N = 3;
velOpt = 6;
velDes = 20;
ReOptimize = zeros(120,4);
ReDesign = zeros(120,4);
filename = 'Step 2 Local Reynolds Number Values and Averaging Scheme
Optimization Point.xlsx';
filename2 = 'Step 2 Local Reynolds Number Values and Averaging Scheme
Design Point.xlsx';
%Re(1,1) = 'Chord';
%Re(1,2) = 'TSR';
%Re(1,3) = 'Reynolds Number';
n = 0;
for c = 0.035:0.035:0.175
    for x = 0.5:0.5:12
        n = n+1;
        ReOptimize(n,1) = c;
        ReOptimize(n,2) = x;
        ReOptimize(n,3) = abs((((x*velOpt)*c)/nu)*(sqrt(x^2+1))/x); %at
0 deg
        ReOptimize(n,4) = abs((((x*velOpt)*c)/nu)*(x-1)/x); %at 90 deg
        ReDesign(n,1) = c;
        ReDesign(n,2) = x;
        ReDesign(n,3) = abs((((x*velDes)*c)/nu)*(sqrt(x^2+1))/x); %at 0
deg
        ReDesign(n,4) = abs((((x*velDes)*c)/nu)*(x-1)/x); %at 90 deg
    end
end
xlswrite(filename,ReOptimize);
xlswrite(filename2,ReDesign);
```

Similarly, upwind and downwind angle of attacks were calculated using the following code:

```
clear all; clc;
%Upwind angle of attacks
filename = 'Step 1 Alpha Values Range.xlsx';
UAlpha = zeros(432,7);
n = 0;
for x = 0.5:0.5:12
    for th = 85:-10:-85
        n = n+1;
        UAlpha(n,1) = x;
        UAlpha(n,2) = th;
```

```
        UAlpha(n,3) = round(asind((cosd(th))/(sqrt((x-sind(th))^2 +
(cosd(th))^2))),2);
    end
end
%Downwind angle of attacks
n = 0;
for x = 0.5:0.5:12
    for th = 95:10:265
        n = n+1;
        UAlpha(n,5) = x;
        UAlpha(n,6) = th;
        UAlpha(n,7) = round(asind((cosd(th))/(sqrt((x-sind(th))^2 +
(cosd(th))^2))),2);
    end
end
xlswrite(filename,UAlpha);
```

Having determined the ranges of required angle of attack values and operating Reynolds numbers, QBlade v0.963 which is an open source software for wind turbine design and simulation was used to obtain the polars for the Airfoil NACA 0018. The data was exported as txt file and further imported to excel, to later be fed into MATLAB.

The MATLAB code for the DMST adaptation was written, which is given below:

```
clear all; clc; format long;
H = 0.5;  l = 1;  N = 3;  R = 0.5;   S = 1;   den = 1.20; nu =
1.48*10^(-5); %fixed parameters
Vf = 6;
Data1 = xlsread('Data1.xlsx');
Data2 = xlsread('Data2.xlsx');
Data3 = xlsread('Data3.xlsx');
Data4 = xlsread('Data4.xlsx');
Data5 = xlsread('Data5.xlsx');
Data6 = xlsread('DesignPointData.xlsx');
alphaAU = 0; alphaU = 0; Wu = 0; Vu = 0; Cl = 0; Cd = 0; CN = 0; CT =
0; FUP = 0; uini = 1; ufin = 0; %UpwindInitialization
intFac = zeros(4320,7);
k = 0; n = 0; e = 1;
for c = 0.035:0.035:0.175
    for X = 0.5:0.5:12
        TUP = 0;
        for th = 85:-10:-85
            if c == 0.035
                Data = Data1;
            end
            if c == 0.07
                Data = Data2;
            end
            if c == 0.105
                Data = Data3;
```

```
            end
            if c == 0.14
                Data = Data4;
            end
            if c == 0.175
                Data = Data5;
            end
            [q,o] = size(Data);
            alphaAU = round(asind((cosd(th))/(sqrt((X-sind(th))^2 +
(cosd(th))^2))),4);
            diff = zeros(q,1);
            i = 0;
            for j = 1:q
                diff(j,1) = abs(alphaAU-Data(j,1));
            end
            for j = 1:q
                if diff(j,1) == min(diff)
                    i = j;
                end
            end
            alphaU = Data(i,1);
            Cl = Data(i,2);
            Cd = Data(i,3);
            CN = Cl*cosd(alphaU) + Cd*sind(alphaU);
            CT = Cl*sind(alphaU) - Cd*cosd(alphaU);
            while 1
                Vu = uini*Vf;
                Wu = Vu*sqrt((X-sind(th))^2 + (cosd(th))^2);
                funU = @(t) abs(sec(t)).*(CN.*cos(t)-
CT.*sin(t)).*(Wu/Vu).^2;
                intU = integral(funU,-pi/2,pi/2);
                FUP = ((N*c)/(8*pi*R))*intU;
                ufin = pi/(FUP+pi);
                errorU = abs(ufin - uini);
                uini = ufin;
                if errorU <= 10^(-6)
                    break;
                end
            end
            k = k+1;
            uU = ufin;
            intFac(k,1) = c;
            intFac(k,2) = X;
            intFac(k,3) = th;
            intFac(k,4) = uU;
            Vuf = uU*Vf;
            Wuf = Vuf*sqrt((X-sind(th))^2 + (cosd(th))^2);
            FN = (c*H/S)*CN*((Wuf/Vuf)^2);
            FT = (c*H/S)*CT*((Wuf/Vuf)^2);
            intFac(k,5) = FN*(0.5*den*S*(Vf^2));
            intFac(k,6) = FT*(0.5*den*S*(Vf^2));
            Tup = 0.5*den*c*R*H*CT*(Wuf^2);
            intFac(k,7) = Tup;
```

```
            TUP = TUP + Tup;
        end
        k = k+18;
        CQ1 = (TUP/10)/(0.5*den*(Vf^2)*S*R);
        e = e + 10;
    end
end
alphaD = 0; alphaAD = 0; Wd = 0; Ve = 0; Vd = 0; Cld = 0; Cdd = 0; CNd
= 0; CTd = 0; FUPd = 0; %DownwindInitialization
k = 0; t = 18;
Cp = zeros(5,24);
Cq = zeros(5,24);
m = 1;  e = 1; n = 1;
for c = 0.035:0.035:0.175
    for X = 0.5:0.5:12
        TDW = 0;
        for th = 95:10:265
            if c == 0.035
                DataD = Data1;
            end
            if c == 0.07
                DataD = Data2;
            end
            if c == 0.105
                DataD = Data3;
            end
            if c == 0.14
                DataD = Data4;
            end
            if c == 0.175
                DataD = Data5;
            end
            [q,o] = size(DataD);
            alphaAD = round(asind((cosd(th))/(sqrt((X-sind(th))^2 +
(cosd(th))^2))),4);
            diffd = zeros(q,1);
            i = 0;
            for j = 1:q
                diffd(j,1) = abs(alphaAD-DataD(j,1));
            end
            for j = 1:q
                if diffd(j,1) == min(diffd)
                    i = j;
                end
            end
            alphaD = DataD(i,1);
            Cld = DataD(i,2);
            Cdd = DataD(i,3);
            CNd = Cld*cosd(alphaD) + Cdd*sind(alphaD);
            CTd = Cld*sind(alphaD) - Cdd*cosd(alphaD);
            k = k+1;
            t = t+1;
            uaux = intFac(k,4);
```

```
            Ve = (2*uaux-1)*Vf;
            uinid = uaux;
            while 1
                Vd = uinid*Ve;
                Wd = Vd*sqrt((X-sind(th))^2 + (cosd(th))^2);
                funD = @(td) abs(sec(td)).*(CNd.*cos(td)-
CTd.*sin(td)).*(Wd/Vd).^2;
                intD = integral(funD,pi/2,3*pi/2);
                FDW = ((N*c)/(8*pi*R))*intD;
                ufind = pi/(FDW+pi);
                errorD = abs(ufind - uinid);
                uinid = ufind;
                if errorD <= 10^(-6)
                    break;
                end
            end
            uD = ufind;
            intFac(t,1) = c;
            intFac(t,2) = X;
            intFac(t,3) = th;
            intFac(t,4) = uD;
            Vdf = uD*Ve;
            Wdf = Vdf*sqrt((X-sind(th))^2 + (cosd(th))^2);
            FNd = (c*H/S)*CNd*((Wdf/Vdf)^2);
            FTd = (c*H/S)*CTd*((Wdf/Vdf)^2);
            intFac(t,5) = FNd*(0.5*den*S*(Vf^2));
            intFac(t,6) = FTd*(0.5*den*S*(Vf^2));
            Tdw = 0.5*den*c*R*H*CTd*(Wdf^2);
            intFac(t,7) = Tdw;
            TDW = TDW + Tdw;
        end
        k = k+18;
        t = t+18;
        CQ2 = (TDW/10)/(0.5*den*(Vf^2)*S*R);
        n = n+1;
        e = e + 10;
    end
    m = m+1;
end
xlswrite('Step 3 Complete Analysis 18 tubes.xlsx',intFac);
```

A unique averaging scheme was used to calculate the COP from the results obtained through the above mentioned code, the excel file was first sorted by replacing the negative values of azimuthal with an angle in the range 0 to 360°. After that the data was sorted in ascending order with respect to the azimuthal angle, for each value of solidity and TSR. The code then used to calculate COP at different chords is given below:

```
clear all; clc; format long;
file = xlsread('Step 3 Complete Analysis 18 tubes sorted.xlsx');
```

```
file1 = zeros(4320,8);
i = 1; p = 0; m = 1;
for c = 0.035:0.035:0.175
    for X = 0.5:0.5:12
        data = file(i:i+35,:);
        for j = 1:36
            p = p+1;
            k = j+12;
            if k > 36
                k = k-36;
            end
            l = k+12;
            if l > 36
                l = l-36;
            end
            totalmoment = data(j,7) + data(k,7) + data(l,7);
            file1(p,1) = file(p,1);
            file1(p,2) = file(p,2);
            file1(p,3) = file(p,3);
            file1(p,4) = file(p,4);
            file1(p,5) = file(p,5);
            file1(p,6) = file(p,6);
            file1(p,7) = file(p,7);
            file1(p,8) = totalmoment;
        end
        i = i+36;
    end
end
xlswrite('Step 4 COP Calcultions.xlsx',file1);
CP = zeros(5,24);
i = 1; m = 1;
for c = 0.035:0.035:0.175
    n = 1;
    for X = 0.5:0.5:12
        data = file1(i:i+35,8);
        CP(m,n) = (mean(data)/10.8)*X;
        i = i+36;
        n = n+1;
    end
    m = m+1;
end
xlswrite('Step 5 COP.xlsx',CP);
```

After having chosen one value of chord, the data of the selected chord at the design velocity was separated and stored in a different file.

APPENDIX III: CALCULATIONS

The dimensions of radial arm and shaft are determined by applying radial, tangential and weight forces as found from the DMST model.

Radial force is responsible for compression and tension in the arm and shaft, whereas weight and tangential forces are used to sketch shear force and bending moment diagrams of shaft which ultimately use factor of safety to determine the dimensions of radial arms and shaft.

Radial arm

Normal stress is given by:

$$\sigma = F/A$$

$$\sigma = 230 \text{ MPa}$$

This means a factor of safety of 1.2.

Bending normal stress is given by:

$$\sigma_{max} = \frac{M.c}{I}$$

$$\sigma_{max} = 110 \text{ MPa}$$

Factor of safety is given by:

$$FOS\ \sigma = \frac{\sigma_y}{\sigma_{allowable}}$$

It turns out to be around 2.5. This shows that the design is safe.

Shear stress is given by:

$$\tau_{max} = \frac{V.Q}{I.t}$$

$$\tau_{max} = 3 \text{ MPa}$$

$$FOS\ \tau_{max} >> 50$$

Therefore, shear stress is well controlled.

Buckling is given by:

$$P_{cr} = \frac{\pi^2 EI}{(KH)^2}$$

Moment of inertia of tube is given by:

$$I = \pi (d_o^4 - d_i^4) / 64$$

Buckling is the deciding factor because it results in the minimum safety factor of 1.1, the dimensions of our radial arm turn out to be:

Outer diameter = 1 inch

Tube thickness = 0.0625 inch

Shaft

Since three radial arms are attached with the shaft, three instantaneous maximum forces are used to determine the diameter of shaft. The shear force and bending moment diagrams are drawn below:

Shear Force and Bending Moment Diagram of shaft at radial force of 633 N:

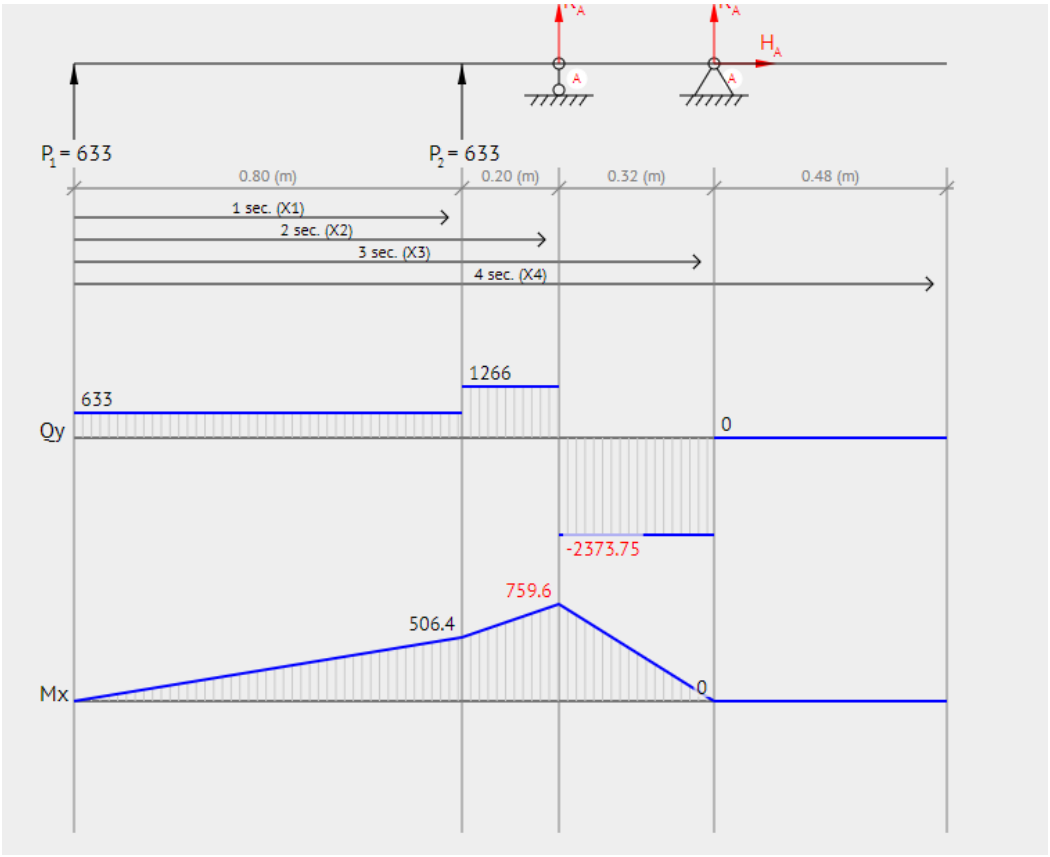

Shear Force and Bending moment diagram of shaft at radial force of 415 N.

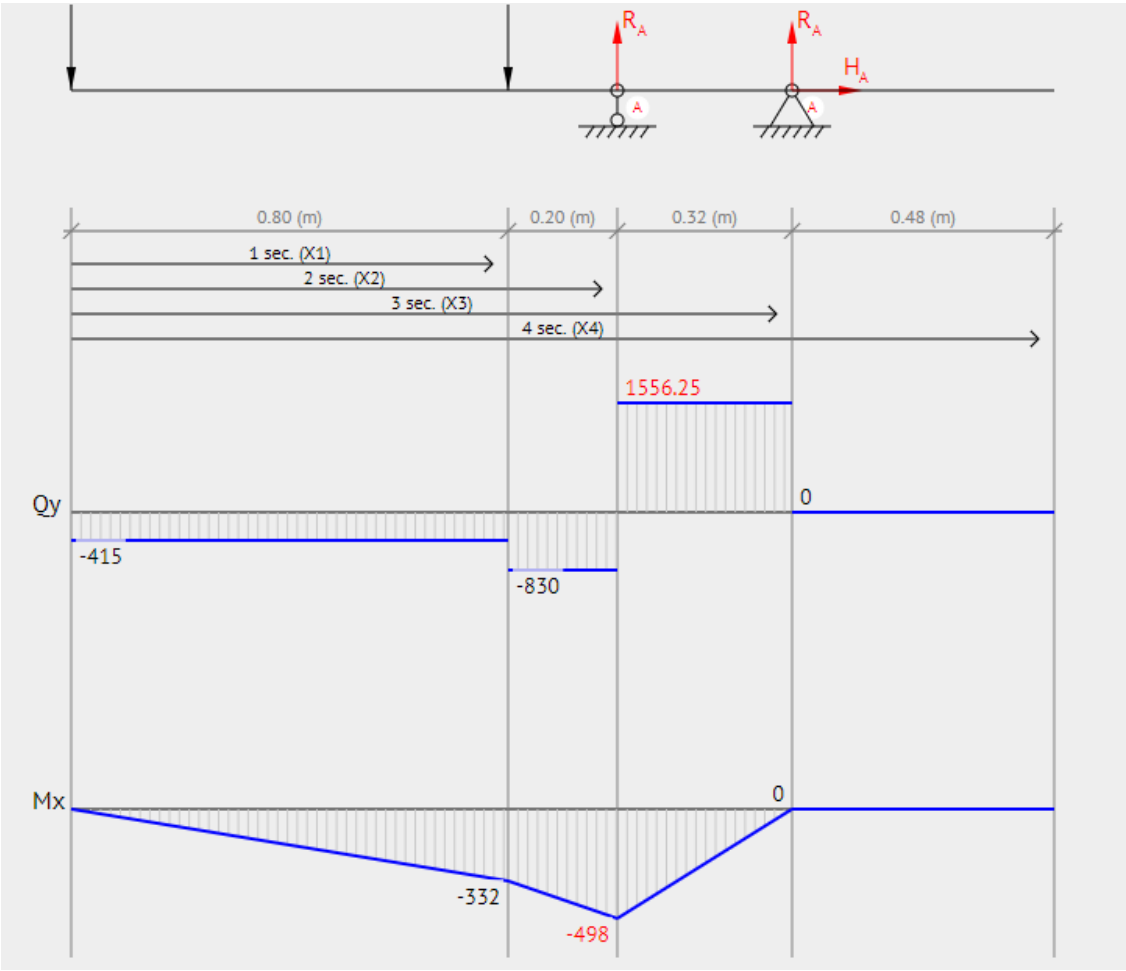

Shear Force and Bending moment diagram of shaft at radial force of 200 N.

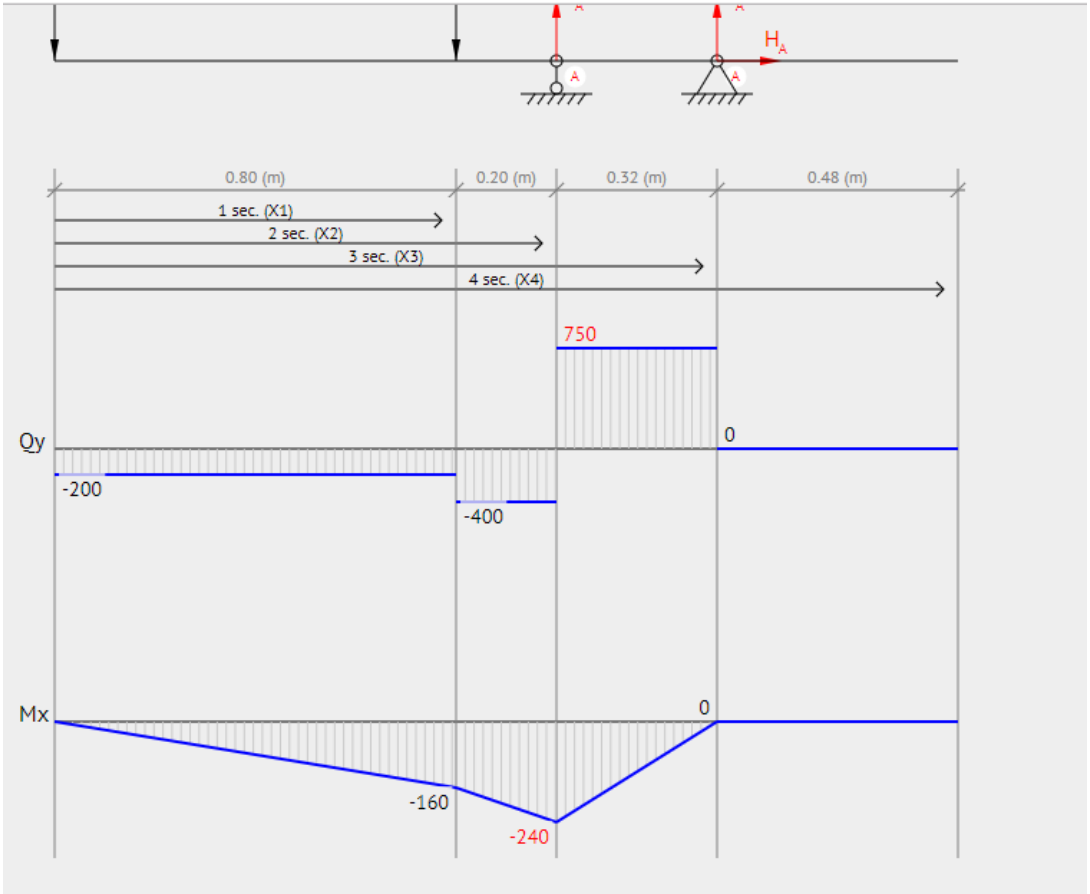

Normal stress is given by:

$$\sigma = Mc/I$$

This results a factor of safety of 1.4.

Shear stress is given by:

$$\tau_{max} = \frac{V.Q}{I.t}$$

$$\tau_{max} = 8 \text{ MPa}$$

$$\text{FOS } \tau_{max} >> 30$$

Therefore, shear stress is well controlled. The diameter of shaft comes out to be 3 cm.

Bearing

An SKF manual for bearings was studied. Different types of bearings have their own specialty. After thorough research, deep groove ball bearing was selected. SKF have a special class of energy efficient bearings. Our forces and outer diameter of shaft were the main consideration during the bearing selection process.

Equivalent load on the bearing is given by:

$P = XVF_r + YF_a$

V=1

Through calculations:

X=0.46

Y=1.67

Radial force, Fr = 4 kN

Axial force, F_a = 2 kN

Subsequently, P = 4 kN

Principal Dimensions			Basic Static	Dynamic load	Fatigue load	Model
d (mm)	D (mm)	B (mm)	C (kN)	C_o (kN)	P (kN)	
30	55	13	12.7	7.35	0.31	E2.6006
30	62	16	19.5	11.2	0.475	E2.6206
30	72	19	28.6	16	0.67	E2.6306

Based on the above data, the energy efficient, 6206-2Z was selected.

APPENDIX IV: FRAME STRESS ANALYSIS USING ANSYS

The stress analysis of the frame was conducted in ANSYS Static Structural module. The results obtained are shown below:

Total Deformation:

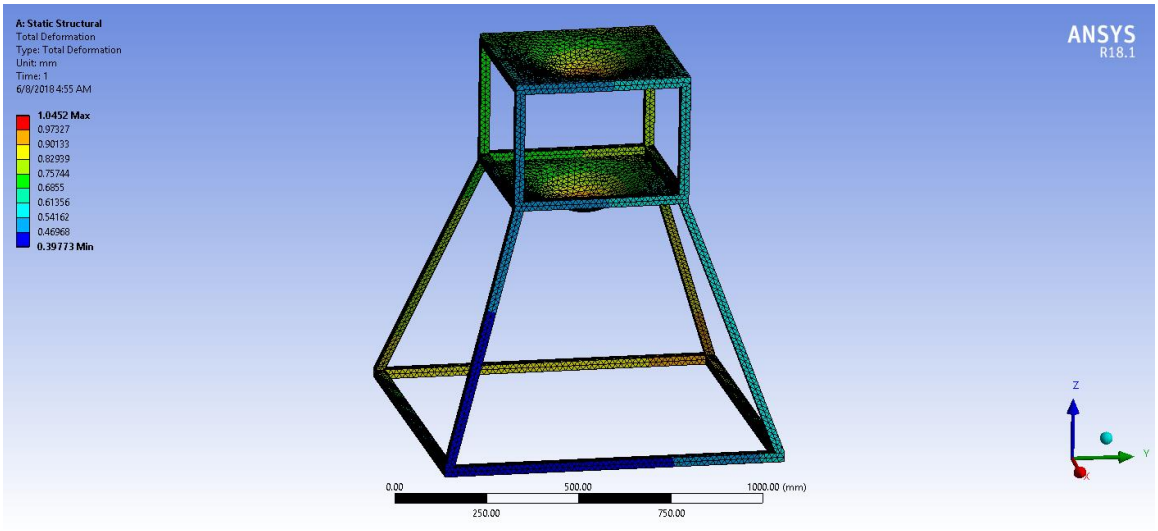

Maximum Principal Stress: